Palaeogeography, Palaeoclimatology, Palaeoecology 406 (2014) 1–8

Contents lists available at ScienceDirect

Palaeogeography, Palaeoclimatology, Palaeoecology

journal homepage: www.elsevier.com/locate/palaeo

Refining the pedogenic carbonate atmospheric CO_2 proxy and application to Miocene CO_2

D.O. Breecker [a,*], G.J. Retallack [b]

[a] Department of Geological Sciences, The University of Texas at Austin, Austin, TX, United States
[b] Department of Geological Sciences, The University of Oregon, Eugene, OR, United States

ARTICLE INFO

Article history:
Received 8 February 2014
Received in revised form 12 April 2014
Accepted 16 April 2014
Available online 26 April 2014

Keywords:
Paleoatmospheric CO_2
Paleosol
Miocene
Carbon isotopes
Uncertainty
Earth system sensitivity

ABSTRACT

Quantifying uncertainty is essential for any paleoenvironmental proxy. Recent work on propagating error through the equation used to determine atmospheric CO_2 concentrations from paleosol carbonates yields conflicting results. Small magnitude uncertainty from Gaussian error propagation contrasts with larger magnitude uncertainty from Monte Carlo error propagation. The discrepancy is reconciled here by revising partial differential equations for the Gaussian approach. Uncertainties calculated using the two approaches are compared and applied to Miocene calcic paleosols. Monte Carlo-propagated errors are asymmetrical but otherwise agree with Gaussian errors. Three methods for assigning soil-respired CO_2 concentrations ($S(z)$) to paleosols are also compared. A revised calibration of depth to the Bk horizon as a direct proxy for $S(z)$ is presented and although it results in lower atmospheric CO_2 concentrations than the original calibration, it results in significantly higher calculated atmospheric CO_2 than the use of mean annual precipitation as a proxy for $S(z)$ or assigning $S(z)$ values based on soil order. Averaging atmospheric CO_2 concentrations calculated using soil-order based $S(z)$ values from >10 penecontemporaenous and independent paleosols will likely result in useful constraints on Earth system sensitivity. The improvement of proxies for $S(z)$ is needed to increase the accuracy and precision and to resolve potential volatility in CO_2 time series.

1. Introduction

With atmospheric CO_2 peaking at 400 ppm in May 2013 (Tans and Keeling, 2013) and strongly linked with human emissions and global warming (Stocker et al., 2013) Earth's ancient greenhouse climates are becoming increasingly realistic analogs for our future. Computer models used for projections of future climate have been able to accurately simulate rapid feedbacks (<10 years) for several decades (Charney, 1979). In order to accurately simulate longer timescale feedbacks and thereby project warming over longer timescales, these models need to be tested using proxy data, including atmospheric CO_2 concentrations, from ancient warm episodes (e.g. Lunt et al., 2010; Naish and Zwartz, 2012; Royer et al., 2012; Pierrehumbert, 2013; Schmidt et al., 2013). In addition to validating climate models, paleoatmospheric CO_2 records also help quantify Earth's geologic carbon cycle and how it responds to both slow and rapid perturbation (e.g. Berner, 2006; Schaller et al., 2011). Paleoatmospheric CO_2 concentrations can be calculated using measured differences between the $\delta^{13}C$ values of calcium carbonate and organic matter preserved in paleosols (Cerling, 1991). Abundant, high-resolution sequences of paleosols in the terrestrial rock record make these materials attractive for paleoclimate work, because of their potential for time series of high temporal resolution (Retallack et al., 2004; Retallack, 2009b). As for any paleoenvironmental proxy, accurate propagation of error is required to draw statistically significant conclusions regarding, for instance, trends in atmospheric CO_2 or Earth system sensitivity (ESS, Hansen et al., 2008; Lunt et al., 2010). Two recently applied methods of error propagation through Cerling (1999) pedogenic carbonate paleobarometer are Gaussian (Retallack, 2009b) and Monte Carlo simulation (Breecker, 2013), but these give different magnitudes of error, a discrepancy that is reconciled here.

The least well constrained input for the Cerling (1999) paleobarometer is soil respired CO_2 concentration ($S(z)$), which is highly variable in both space and time (Breecker et al., 2009, 2013). Proxies for $S(z)$ include the depth to salts (Retallack, 2009b) and mean annual precipitation (MAP) (Cotton and Sheldon, 2012). It has also been argued that $S(z)$ values can be assigned based on soil order (Breecker, 2013; Montañez, 2013). These three approaches for assigning $S(z)$ are compared here by application to Miocene paleosols from Montana (Cotton and Sheldon, 2012), midwestern United States (Fox and Koch, 2003) and Rusinga Island, Kenya (Bestland and Krull, 1999).

* Corresponding author at: The University of Texas at Austin, Department of Geological Sciences, Dan Breecker, 2275 Speedway Stop C9000, Austin, TX 78712 – 1722. Tel.: +1 512 471 6166; fax: +1 512 471 0959.
E-mail address: breecker@jsg.utexas.edu (D.O. Breecker).

http://dx.doi.org/10.1016/j.palaeo.2014.04.012
0031-0182/

2. Background

2.1. The paleosol carbonate atmospheric CO_2 proxy

The equation relating atmospheric CO_2 concentrations with the carbon isotope compositions of soil carbonate and soil respired CO_2 is as follows (Cerling, 1999):

$$[CO_2]_{atm} = S(z)R = S(z)\frac{\delta^{13}C_s - 1.0044\delta^{13}C_r - 4.4}{\delta^{13}C_a - \delta^{13}C_s} \quad (1)$$

where $[CO_2]_{atm}$ is the atmospheric CO_2 concentration and $S(z)$ is the concentration of soil CO_2 that is contributed by soil respiration (i.e. $S(z)$ = soil CO_2 concentration − $[CO_2]_{atm}$). The variable S varies with depth (z) and with time, here we are concerned with S at the depth of carbonate formation and at the time of year of carbonate formation. In Eq. (1), $\delta^{13}C$ represents the carbon isotope composition expressed in the standard per mil notation and the subscripts s, r and a refer to soil CO_2, soil-respired CO_2 and atmospheric CO_2 respectively. The variable R equals the fraction involving the $\delta^{13}C$ values on the right hand side of Eq. (1). This equation derives from isotope mass balance and the concept that CO_2 in soils is a mixture between atmospheric CO_2 and CO_2 produced in the soil by biological respiration. Values of $\delta^{13}C_a$ can be calculated from marine foraminiferal records (Passey et al., 2002) and are available throughout the Cenozoic (Tipple et al., 2010). For application to paleosols, the carbon isotope composition of respired CO_2 is best determined from the carbon isotope composition of soil organic matter (Cerling, 1992). It is well documented that $\delta^{13}C$ values of organic matter in modern soils are similar to litter near the surface and increase with depth (e.g. Feng et al., 1999; Wynn et al., 2005; Wynn and Bird, 2007), even in soils that were archived before substantial onset of the Seuss effect (Torn et al., 2002). Therefore organic carbon in soil B horizons, which are typically sampled when working with paleosols, has $\delta^{13}C$ values higher than the average biomass. It has therefore been suggested that measured $\delta^{13}C$ values of B horizon soil organic matter be accordingly adjusted in order to accurately determine $\delta^{13}C_r$ for use in Eq. (1) (Bowen and Beerling, 2004; Breecker, 2013). The equation $\delta^{13}C_r = \delta^{13}C_{om} - 1$, where '*om*' is paleosol organic matter, is used here.

The carbon isotope composition of CO_2 in soil pore spaces during carbonate formation ($\delta^{13}C_s$) can be determined from the carbon isotope composition of paleosol carbonates and the temperature of their formation (Cerling, 1991) using the temperature-sensitive equilibrium isotope fraction factor between calcite and CO_2 (Romanek et al., 1992):

$$\delta^{13}C_s = \frac{\delta^{13}C_{cc} + 1000}{\frac{(11.98 - 0.12T)}{1000} + 1} - 1000 \quad (2)$$

which can be substituted into Eq. (1) for error propagation. Determination of the temperature of formation can be difficult for several reasons. Oxygen isotope compositions of pedogenic carbonates can be a guide, but require calibration for latitude, elevation and distance from the ocean (Dworkin et al., 2005; Kent-Corson et al., 2006), and are prone to diagenetic and metamorphic resetting in deep time (Mora et al., 1998). Other methods of calculating paleotemperatures from chemical composition of paleosols give the mean annual temperature (Gallagher and Sheldon, 2013), but in most soils carbonate precipitates preferentially in the warm season (Breecker et al., 2009; Passey et al., 2010; Quade et al., 2013). Some low elevation (>2 km) soils in summer wet parts of South America are exceptions in that carbonates record the mean annual temperature (Peters et al., 2013). These exceptions were discovered with the clumped isotope thermometer (Ghosh et al., 2006), which gives the most reliable temperatures for use in calculating $\delta^{13}C_s$ in paleosols that have been shallowly buried (Quade et al., 2013). Each of these temperature proxies have error envelopes that also need to be introduced into Eq. (1).

2.2. Quantifying $S(z)$

Four principal approaches have been used for quantifying values of $S(z)$: 1) soil categories (Cerling, 1991); 2) soil orders (Montañez, 2013); 3) paleoprecipitation (Cotton and Sheldon, 2012); and 4) calcic-depth (Retallack, 2009b). The original values used by Cerling (1991) varied from below 3000 to 10,000 ppmV and were based on whether there was evidence for soils having formed in deserts (below 3000 ppmV) or whether the soils were well drained and formed in temperate or tropical climates (5000–10,000 ppmV). Different values, also based on soil morphology, were used by Montañez et al. (2007). A single lower $S(z)$ value (2500 ppmV) was proposed to be appropriate for averages of large numbers of paleosols (Breecker et al., 2010), based on solving Eq. (1) for $S(z)$ and applying to modern surface soils using preindustrial values for atmospheric CO_2. Soil order-based $S(z)$ values have recently been tabulated (Montañez, 2013) and revised using the same method (Breecker, 2013). The primary advantage of the soil order approach over the soil category approach is increased specificity, there being a significant difference in $S(z)$ among some soil orders (Breecker, 2013). The advantages of the soil order approach over the paleoprecipitation and calcic-depth approaches (described below) involves the method by which each has been calibrated. First, the soil order based approach has been calibrated using 202 soils whereas the paleoprecipitation and calcic-depth proxy calibrations involve only 23 and 15 soils. Second, the soil order approach is calibrated by solving Eq. (1) for $S(z)$ and applying to modern soils, which inevitably results in $S(z)$ values that are appropriate in Eq. (1) because they correspond to carbonate accumulation. This is not necessarily the case for the existing paleoprecipitation and calcic-depth proxy calibrations. These proxies have been calibrated by assuming that the warm season minimum (Cotton and Sheldon, 2012) or late growing season shoulder (Retallack, 2009b) $S(z)$ values correspond to carbonate accumulation. The measurements of soil $S(z)$ in these studies were made during relatively short-duration (i.e. 1 or 2 growing seasons) and in some cases low temporal resolution (as low as only 1 growing season measurement) soil gas monitoring studies. If calcite primarily accumulates in soils during sporadic droughts (i.e. not every year, Breecker et al., 2009), then the gas monitoring studies used for calibration may not have captured carbonate accumulation events and the $S(z)$ values used for calibration may be overestimates. Alternatively, carbonate in some of the soils used for the paleoprecipitation and calcic-depth calibrations may have formed at a different time of year than was assumed. Both of these could result in inaccurately assigned $S(z)$ values, given that soil CO_2 concentrations vary seasonally and interannually (see compilation of seasonal variations in Retallack, 2009b; Breecker et al., 2013). It should be noted, however, that Eq. (1) was used to validate the paleoprecipitation proxy for $S(z)$ (Cotton and Sheldon, 2012).

Although calibration by solving Eq. (1) for $S(z)$ circumvents these potential shortcomings it also involves a number of complexities and drawbacks of its own. Comparison between $\delta^{13}C$ values of soil organic matter and soil carbonate measured in modern surface soils requires consideration of the Seuss effect (impacts on both organic matter and carbonate may be minimal in the B horizon). The relatively low modern atmospheric pCO_2 theoretically results in a large error for $S(z)$ > 600 ppmV (Breecker, 2013). Furthermore, soil order explains little of the $S(z)$ variance in Mollisols, Aridisols and Alfisols (there are no significant differences in $S(z)$ among these soil orders, Breecker, 2013) indicating that this categorical approach misses the main controls on $S(z)$, which has also been concluded for mean summer $S(z)$ (Cotton et al., 2013). Precision might therefore be improved by using different or additional categories or using continuously variable proxies. Although the soil-order approach accounts for variance of $S(z)$ within soil orders (the variance is considered as an error that is propagated

through Eq. (1)), it does not resolve such variations and therefore, when applied to sequences of paleosols, may attenuate the actual secular variations in atmospheric CO_2. Finally, it should be noted that $S(z)$ varies widely both spatially and temporally in Vertisols (Breecker et al., 2013) and therefore uncertainty associated with $S(z)$ for Vertisol and other soils with vertic properties is currently large.

Two other proxies for $S(z)$ are continuous variables and are therefore perhaps better suited to the study of time-series. The first relates $S(z)$, measured in modern soil pore spaces at the end of the growing season, to the depth of the soil horizon in which calcium carbon accumulates, the Bk horizon (Retallack, 2009b). The standard error (se) associated with the transfer function for $S(z)$ from modern soils is ±766 ppm for carbonate and ± 659 ppm for gypsum. The second relates $S(z)$, again measured in soil pore spaces, to mean annual precipitation (Cotton and Sheldon, 2012), which in turn is related to depth to Bk (e.g. Retallack, 2005) or to chemical weathering indices such as, CIA-K (Sheldon et al., 2002) or CALMAG (Nordt and Driese, 2010). The standard error for $S(z)$ determined from the modern transfer function of Cotton and Sheldon (2012) is ±681 ppm. Total $S(z)$ error is larger than this because uncertainty in determination of paleoprecipitation needs to be incorporated and this is significant: se = ±147 mm for depth to Bk (Retallack, 2005), se = ±172 mm for CIA-K (Sheldon et al., 2002) and se = ±108 mm for CALMAG (Nordt and Driese, 2010). The primary advantage of the calcic depth and paleoprecipitation proxies is the potential to distinguish variations in $S(z)$ within and among soil orders and other categories, which may be important for resolving CO_2 spikes in the geologic record. It should be noted that these proxies could be calibrated by rearranging Eq. (1) (rather than using measured pore space CO_2 concentrations). The soil order, paleoprecipitation and calcic-depth (after revision, see below) approaches are compared here in their application to Miocene paleosols.

3. Methods

The equation used for Gaussian error propagation is based on a Taylor series expansion of the function of interest, f(x,y,z …) and relates total error associated with the value of a function (i.e. error on the value of f) to error on each of the variables (x,y,z…):

$$s_f = \sqrt{\left(\frac{\partial f}{\partial x}\right)^2 s_x^2 + \left(\frac{\partial f}{\partial y}\right)^2 s_y^2 + \left(\frac{\partial f}{\partial z}\right)^2 s_z^2 + \cdots} \quad (3)$$

where s_f represents the total error (standard deviation of the values of f), s_x, s_y, s_z… represent the standard deviations of each input variable, and $\frac{\partial f}{\partial x}, \frac{\partial f}{\partial y}, \frac{\partial f}{\partial z}$… are the partial derivatives of f with respect to each input variable. Eq. (3) is a good approximation if the standard deviations of input variables are small relative to the partial derivatives (Clifford, 1973). The relevant equation for error associated with atmospheric CO_2 concentrations determined using calcic paleosols is:

$$S_{[CO_2]_{atm}} = \sqrt{\left(\frac{\partial [CO_2]_{atm}}{\partial S(z)}\right)^2 S_{S(z)}^2 + \left(\frac{\partial [CO_2]_{atm}}{\partial \delta^{13}C_s}\right)^2 S_{\delta^{13}C_s}^2 + \left(\frac{\partial [CO_2]_{atm}}{\partial \delta^{13}C_r}\right)^2 S_{z\delta^{13}C_r}^2 + \left(\frac{\partial [CO_2]_{atm}}{\partial \delta^{13}C_a}\right)^2 S_{z\delta^{13}C_a}^2}. \quad (4)$$

Eq. (4) can be further expanded by replacing the $\delta^{13}C_s$ term with terms for the $\delta^{13}C$ value of pedogenic carbonate and the temperature of soil carbonate formation, which are together used to calculate $\delta^{13}C_s$ (see Retallack, 2009b for the expanded equation). The expanded version of Eq. (4) was used to calculate the errors reported here. Additional substitutions are appropriate wherever one of the variables in Eq. (4) is calculated from values of other variables. The equations for each of the partial derivatives in the expanded version of Eq. (4) are shown in the Supplementary data and an Excel spreadsheet incorporating these equations is available from the authors.

Monte Carlo error propagation involves randomly selecting values from normal (or other) distributions defined for each variable on the right hand side of Eq. (1). A value for $[CO_2]_{atm}$ is calculated using the randomly selected values. This process is repeated some large number of times (10,000 iterations used here), resulting in a distribution of $[CO_2]_{atm}$ from which mean, median, percentile values, etc. can be calculated. The Matlab code PBUQ (Breecker, 2013) was used to carry out the Monte Carlo error propagation. The 84th and 16th percentile values (i.e. middle 68%) from the Monte Carlo simulations are reported for comparison with standard deviations from the Gaussian approach.

Gaussian error propagation assumes independence of variables. The variables in Eq. (1) used to calculate paleoatmospheric CO_2 are not mechanistically independent, as noted by Breecker (2013). For instance, $\delta^{13}C_r$ is related to $\delta^{13}C_a$ because plants get carbon from the atmosphere. Certainly if $\delta^{13}C_r$ was calculated from $\delta^{13}C_a$, then the errors on these variables would be correlated and Gaussian error propagation would be inappropriate (it would underestimate uncertainty on CO_2). However, in this study $\delta^{13}C_r$ is calculated from measured $\delta^{13}C$ values of organic mater occluded in the paleosol carbonate nodules whereas $\delta^{13}C_a$ is calculated from marine foraminifera. This is done because $\delta^{13}C_a$ is not the only control on $\delta^{13}C_r$ and therefore $\delta^{13}C$ values of paleosol organic matter more accurately record $\delta^{13}C_r$ than do values of $\delta^{13}C_a$. Therefore although $\delta^{13}C_r$ and $\delta^{13}C_a$ are not truly independent variables, they are calculated using independently measured variables. Therefore, there is no reason to suspect that the errors on $\delta^{13}C_a$ and $\delta^{13}C_r$ resulting from 1) analytical uncertainty or 2) calculation of the variables of interest from the measured values (e.g., calculation of $\delta^{13}C_a$ from $\delta^{13}C$ of marine foraminifera) are correlated. However, error on $d^{13}C_r$ and $d^{13}C_a$ resulting from secular changes during an interval of interest are likely to be correlated. Such an error is small and has not been considered here in either the Monte Carlo approach or the inappropriateness of the Gaussian approach.

In order to calculate MAP (the independent variable) from depth to Bk (dependent on MAP), a regression of ln(depth to Bk) on MAP was used (Breecker, 2013). This avoids a bias toward low depth to Bk at low MAP that is introduced when the regression is done with MAP on the y-axis (i.e. regression of MAP on depth to Bk as reported by Retallack, 2005). However regression of ln(depth to Bk) on MAP also results in calculation of negative MAP values when measured depth to Bk is smaller than 20 cm and also likely overestimates MAP when depth to Bk exceeds 1 m. Because the form of the relationship between MAP and depth to Bk is not known a priori, fitting a curve to these data may be most accurately accomplished using monotone smoothing functions, as employed by Beerling et al. (2009) for the relationship between stomatal index and CO_2.

The transfer function in PBUQ (Breecker, 2013) used to calculate $S(z)$ directly from depth to Bk was calculated with $S(z)$ as an independent variable (on the x axis) and Bk on the y axis. This is probably not the best way to do the regression because most of the error is associated with $S(z)$ and it is not clear that either of these variables is truly dependent on the other. More likely both variables are controlled by interactions among other variables such as precipitation, potential evapotranspiration, soil texture and organic matter content. The calculations made here use the original transfer function reported by Retallack (2009b) such that all deviations from the regression line are assumed to be associated with $S(z)$ error.

Error calculations were performed for Miocene paleosols in which $\delta^{13}C$ values of carbonate nodules and B-horizon organic matter have been measured previously. These carbon isotope data were compiled from a number of publications concerning paleosols exposed in Montana (Cotton and Sheldon, 2012), the Great Plains of the United States (Fox and Koch, 2003) and Rusinga Island, Kenya (Bestland and Krull, 1999). Ages used here are as reported or referenced in those publications. Paleosols with organic matter $\delta^{13}C$ values greater than −22‰, which constitutes a likely C_4 biomass component, were not used. Values for the carbon isotope composition of soil respired CO_2 were calculated using $\delta^{13}C_r = \delta^{13}C_{om} - 1$ (Breecker, 2013). Paleotemperature (mean

annual air temperature) was assumed to be similar to modern and was estimated based on data from nearby cities with an error (1σ) of ± 5 °C assumed. Miocene temperatures probably were not the same as modern, but a conservative error is assigned to these temperature estimates and the calculation of $[CO_2]_{atm}$ is, for most soils, largely insensitive to temperature. Paleotemperature for the Montana paleosols is from Retallack (2007) and is the same value used by Cotton and Sheldon (2012). Soil carbonate formation temperature for low latitude samples (Kenyan paleosols) were set equal to the mean annual temperature (Passey et al., 2010). Soil carbonate formation temperatures for mid latitude samples (Texas, New Mexico, Nebraska) were calculated from assumed mean annual air temperature using a relation resulting from compilation of data from Quade et al (2013) and Passey et al (2010):

$$T = 0.5(MAAT) + 18.0 \quad (5)$$

where T (°C) is the temperature of carbonate formation and MAAT (°C) is the mean annual air temperature. Soil carbonate formation temperatures approximately 15 °C above mean annual air temperatures have recently been reported for modern soils in Wyoming and Nebraska (Hough et al., 2014), including densely vegetated surfaces. This supports the soil carbonate formation temperatures used here which are substantially higher than previous studies of the same paleosols (e.g. Cotton and Sheldon, 2012). Uncertainty would likely be reduced and accuracy improved by measuring the clumped isotope compositions of the paleosol carbonates used in this study. Applying these conventions for calculating $\delta^{13}C_r$ and carbonate formation temperature to the modern soil data used in Breecker et al. (2010) decreases the mean $S(z)$ value from 2800 ± 1800 to 950 ± 300 ppmV, a value consistent with subsequent soil order calibrations (Breecker, 2013; Montañez, 2013).

For the purpose of assigning $S(z)$ values, Alfisols were recognized by subsurface accumulation of clay qualifying as an argillic horizon (Soil Survey Staff, 2010), and Inceptisols were recognized as thick profiles with soil development short of both argillic and calcic horizons. Soils with vertic properties were recognized by the preservation of slickensides and wedge-shaped peds. Vertic Inceptisols exposed on Rusinga Island were classified as Vertisols for the purpose of assigning $S(z)$. Paleosols in which carbonate accumulation was a dominant feature were identified as Aridisols if there was no evidence for a mollic epipedon or as Mollisols if a mollic epipedon was documented. The difference between mean $S(z)$ values in Aridisols and Mollisols is not significant (Breecker, 2013), making this distinction of minor importance for the resulting atmospheric CO_2 concentrations.

The calcic-depth proxy for $S(z)$ was revised by relating depth to carbonate to the lowest growing season $S(z)$ values measured in each soil gas monitoring study. The depth to Bk was revised for the Azerbaijani soils in the calibration dataset and two Entisols with shallow accumulations of carbonate on the underside of clasts (Breecker et al, 2009) were added to the calibration dataset. We term this calibration as 'depth to carbonate' rather than 'depth to Bk' because the Entisols included in the dataset have Ck rather than a Bk horizon.

4. Results and discussion

The revised calibration of depth to carbonate as a proxy for $S(z)$ is shown in Fig. 1. The new calibration has a smaller slope than the original calibration (Retallack, 2009b) and is likely a more accurate reflection of $S(z)$ during carbonate formation in soils. It is currently unclear whether this calibration is applicable to all paleosols or only to a certain subset and this approach might be improved with soil order specific calibrations. The proxy would also benefit from the development of a supporting theoretical framework. Application of this proxy to soils with truncated tops would result in underestimates of $S(z)$, which would counteract the potentially overestimated $S(z)$ values used in the calibration. This calibration can be used for soils with depth to Bk less than 20–30 cm as long as the pedogenic carbonates used to determine the $\delta^{13}C$ value of soil CO_2 are sampled from below 30 cm (Cerling, 1991) to maintain consistency with the depth of soil CO_2 concentration measurements used in the calibration (Retallack, 2009b).

Gaussian and Monte Carlo error bars are generally in good agreement (Table A1, Fig. 2). The Monte Carlo error bars are asymmetrical, especially for the soil order-based approach, and typically shorter than the Gaussian error bars on the low end and longer than the Gaussian error bars on the high end. The skew results from skewed distributions of $S(z)$ that are used to calculate $[CO_2]_{atm}$ and from the multiplication of uncertain variables (Breecker et al, 2013). The medians of these skewed distributions are considered to be the best estimates. The Monte Carlo error bars calculated using $S(z)$ from MAP are larger than the corresponding Gaussian error bars because the latter consider only the error associated with regression of $S(z)$ on MAP (Cotton and Sheldon, 2012) whereas the former also consider error associated with the values of MAP determined from depth to Bk. The absolute magnitude of error varies more among paleosols for the soil-order based approach to assigning $S(z)$ values than for the other approaches because the variance of $S(z)$ is much higher for some soil orders (e.g. Vertisols) than

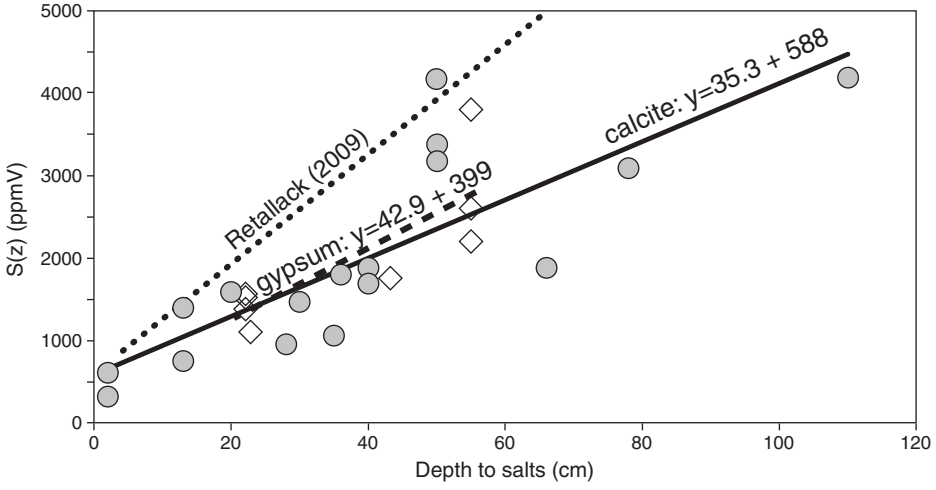

Fig. 1. Calibration of depth to salts as a proxy for $S(z)$. Minimum growing season $S(z)$ values from the data compiled by Retallack (2009b) were used. The calibration reported by Retallack (2009b) for depth to Bk is shown for comparison.

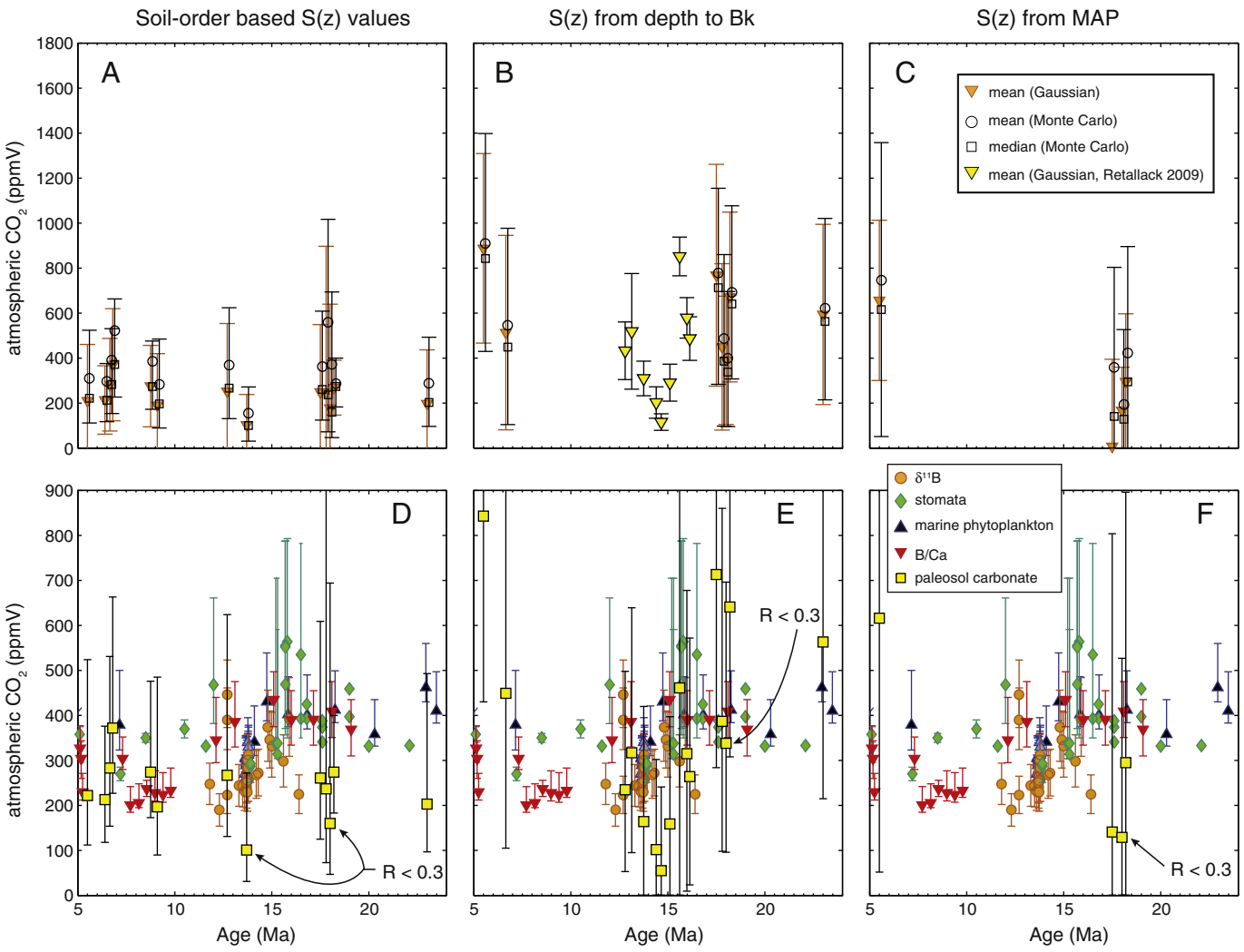

Fig. 2. Proxy-based Miocene atmospheric CO_2 concentrations. Panels in the column on the left, middle and right columns show, respectively, atmospheric CO_2 concentrations determined using soil order-based $S(z)$ values, values from a revised depth to the soil Bk horizon calibration and $S(z)$ values from mean annual precipitation, which was calculated from depth to the soil Bk horizon (Cotton and Sheldon, 2012). The panels in the top row (panels A–C) show comparison between error propagation by Gaussian and Monte Carlo approaches. Orange triangles and error bars show mean values ($\pm 1\sigma$) calculated using Gaussian error propagation. Black symbols show mean (open circles) and median (open squares) values and the black error bars show 16th and 84th percentile values calculated using Monte Carlo error propagation. Atmospheric CO_2 concentrations are displayed for soils with $\delta^{13}C$ values of organic matter less than −22‰ and in B) and C) for soils with measured depth to Bk and for which positive mean $S(z)$ values were calculated. The Kenyan paleosol plotted at 18.1 Ma is constrained to be >18 Ma (Drake et al., 1988). Yellow triangles in B) are from Retallack, 2009b using the original depth to Bk calibration and are shown for comparison. The panels in the bottom row (panels D–F) compare CO_2 determined from other proxies with the CO_2 concentrations determined from paleosol carbonates. The paleosol carbonate values in D–F are medians calculated using the Monte Carlo approach and are duplicated from panels A–C. Atmospheric CO_2 concentrations from Retallack (2009b), adjusted to account for the new calibration of $S(z)$ versus depth to carbonate (Fig. 1), are shown in Panel E. Error bars for these points were calculated assuming ±1‰ on the values of $\delta^{13}C^r$ used by Retallack (2009b). Paleosols for which R < 0.3, unbalanced soils in which $S(z) \gg [CO_2]_{atm}$ resulting in large uncertainty (Breecker, 2013) are indicated. All of the values from Retallack (2009b) have R < 0.3. Miocene atmospheric CO_2 concentrations determined using other proxies are shown for comparison (Van Der Burgh et al., 1993; Kürschner, 1996; Royer et al., 2001; Kürshcner et al., 2008; Beerling et al., 2009; Retallack, 2009a; Tripati et al., 2009; Foster et al., 2012; Badger et al., 2013; Zhang et al., 2013).

others whereas the standard error of $S(z)$ based on regression lines is approximately uniform for all paleosols.

The mean atmospheric CO_2 concentrations calculated using depth to carbonate as a proxy for $S(z)$ are significantly higher than the mean concentrations calculated by assigning $S(z)$ based on soil order (t-test, $p < 0.01$). This discrepancy may derive from different methods of calibration, as described above. Both the depth to carbonate and paleoprecipitation proxies for $S(z)$ result in atmospheric CO_2 concentrations higher than those calculated using the soil order-based approach for the 5.5 Ma paleosols from the Six Mile Creek Formation in Montana (Fig. 2). This discrepancy could be the result of a relatively high $S(z)$ value for this paleosol that is captured by the depth to carbonate but is not well represented by the distribution of $S(z)$ values used in the soil order-based approach. However, the soil order approach results in atmospheric CO_2 concentrations that are more consistent with other proxy records for this soil (Fig. 2). The $[CO_2]_{atm}$ reported here using the $S(z)$ from the MAP technique for the 5.5 Ma Six Mile Creek paleosols is higher than the value reported by Cotton and Sheldon (2012) because a higher carbonate formation temperature and a lower $\delta^{13}C_r$ value were used here. It should be noted that the $S(z)$ from MAP proxy works better when CIA-K, rather than depth to Bk, is used to determine MAP (Cotton and Sheldon, 2012).

Middle Miocene atmospheric CO_2 concentrations (Retallack, 2009b) revised with the new depth to carbonate calibration peak during the middle Miocene thermal maximum (15–17 Ma) and decrease during the middle Miocene climatic transition (14–15 Ma); these trends are consistent with other proxies but some of the best values are unreasonably low (<100 ppmV) (Fig. 2). These atmospheric CO_2 estimates would be improved by measuring the $\delta^{13}C$ values of organic matter in these paleosols outcropping in Railroad Canyon, Idaho and using published

records of $\delta^{13}C_a$ as input for Eq. (1). The error bars on the paleosol-based CO_2 concentrations are larger than the error bars reported for other proxies. It should, however, be recognized that the error bars on the former include all significant sources of error (dominated by $S(z)$) whereas there are unquantified uncertainties associated with some of the other proxies, such as the possible occurrence of carbon concentration mechanisms in marine algae (Zhang et al., 2013) and poor constraints on the variations of sea water $\delta^{11}B$ values during the Cenozoic (Foster et al., 2012).

Given the relatively poor precision on individual CO_2 determinations, can Eq. (1) be usefully applied to Cenozoic climate change? As an example application, we sought to determine whether or not averaging CO_2 concentrations determined from numerous paleosols could help constrain Earth system sensitivity (Hansen et al., 2008; Lunt et al., 2010). Averaging is an appropriate approach for this question because ESS concerns Earth's average atmospheric CO_2 concentration and equilibrium temperature over $>10^3$ years. Therefore the relevant statistic is how well we know the average CO_2 concentration (e.g. standard error of the mean) not how well we know an individual proxy-based determination of atmospheric CO_2 (e.g. standard deviation). Paleosol data from a time slice during which CO_2 was elevated with respect to Late Holocene preindustrial CO_2 are required to calculate the ESS of an elevated CO_2 Earth. Sufficient appropriate paleosol data with which to test such averaging do not currently exist. Therefore, hypothetical paleosols were used in this analysis as a proof-of-concept exercise to determine how many paleosols might need to be averaged for precise ESS determination and thereby whether or not it is feasible to collect the necessary data. The results of our calculations are shown in Fig. 3.

Hypothetical paleosols were considered from a time slice during which atmospheric CO_2 was 2× preindustrial levels (560 ppmV). Realistic 'best' values and uncertainties were chosen for the variables in Eq. (1) (see Fig. 3 caption). The best value for $S(z)$ was assigned either by soil order or, to approximate estimates from depth to Bk, as 2000 ± 780 ppmV (2000 ppmV corresponds to a depth to Bk of 40 cm using the regression line for calcite in Fig. 1) and the best value for $\delta^{13}C_{pc}$ was assigned such that the target CO_2 (560 ppmV) resulted from evaluation of Eq. (1) with the other prescribed best values. Monte Carlo simulations were then used to calculate ESS using the equation:

$$ESS = \frac{\Delta T}{\log_2\left(\frac{CO_2}{280}\right)} \quad (6)$$

where CO_2 is $[CO_2]_{atm}$ calculated for each iteration for the time slice of elevated CO_2, 280 is the late Holocene preindustrial $[CO_2]_{atm}$ (Indermühle et al., 1999) and ΔT is the difference in global mean temperature between the elevated CO_2 time slice and the late Holocene preindustrial period. Errors associated with ΔT were considered in this analysis. For each iteration, the value of ΔT was randomly sampled from a normal distribution for which $1\sigma = \mu/4$ (i.e. assuming that the temperature anomaly can be constrained with and error of ±25% of the mean). For each iteration, between 1 and 50 calculated values of

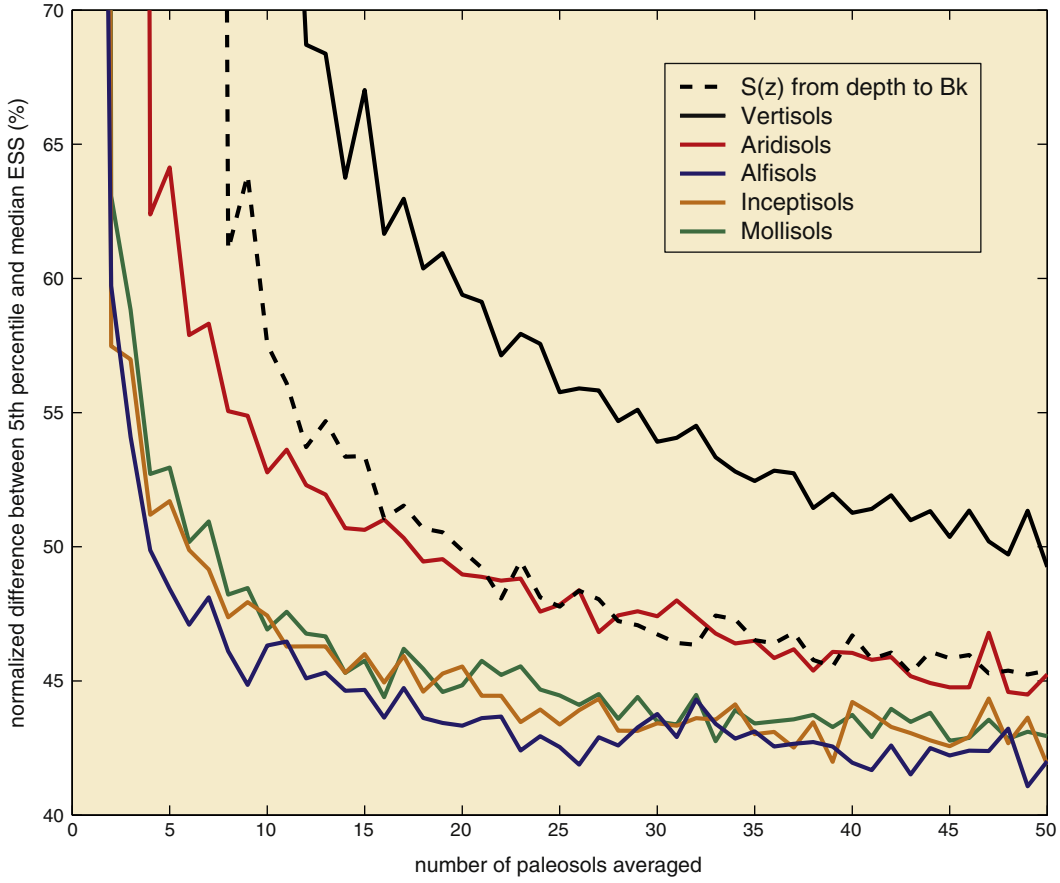

Fig. 3. Relative error associated with Earth system sensitivity (ESS) versus number of paleosols averaged. ESS was calculated as described in the text (Eq. (4)). The following values ($\pm 1\sigma$) were used to calculate $[CO_2]_{atm}$ values during each iteration: 28 ± 5 °C (carbonate formation temperature), −25.0 ± 1.0‰ ($\delta^{13}C_r$), −6.8 ± 0.2‰ ($\delta^{13}C_a$). $S(z)$ assigned by soil order (random sampling from distributions of empirically determined $S(z)$ values, Breecker, 2013; Montañez, 2013) or, to approximate $S(z)$ from depth to Bk, as 2000 ± 780 ppmV. Values of $\delta^{13}C_{pc}$ assigned such that the best value for $[CO_2]_{atm}$ = 560 ppmV. An error of 1σ = 0.75‰ was used for $\delta^{13}C_{pc}$. Averaging among >10 paleosols will likely provide useful constraints on ESS. Averaging among >30 paleosols may not substantially improve precision on ESS. Averaging fewer than 5 paleosols will likely result in highly uncertain ESS estimates.

ESS (to approximate averaging of results from 1 to 50 paleosols) were averaged (median) and the 5th percentile of the resulting distribution of those median ESS values was determined. The normalized difference between the median of the ESS median values and the 5th percentile of the ESS median values:

$$\frac{\text{median of } ESS \text{ medians} - 5\text{th percentile of } ESS \text{ medians}}{\text{median of } ESS \text{ medians}} \cdot 100 \quad (7)$$

is plotted versus the number of paleosols averaged (Fig. 3). This plot shows how the precision on ESS improves with averaging. Minimum ESS (expressed here as the 5th percentile values) are of primary interest here because many other CO_2 proxies saturate at high CO_2 which results in long tails on the low end of estimated ESS distributions. It should be mentioned that 1) ESS determined in this way is not necessarily applicable to projections of future climate due to the state dependency of climate sensitivity (Caballero and Huber, 2013) and that the analysis carried out here does not consider some sources of error such as paleoaltimetry and continental configuration.

Averaging of >10 paleosols constrains the lower error bar on ESS to be 50% of the 'best' value (i.e. if the best estimate for ESS is 3 °C, then there is 95% confidence that ESS > 1.5 °C) which is similar in precision to IPCC summarized constraints on climate sensitivity (Solomon et al., 2007). The CO_2 concentration of the 'elevated CO_2' time slice influences these calculations such that ESS precision increases as the magnitude of the 'elevated CO_2' increases. For practical purposes this necessitates a compromise between more recent warm episodes such as the Middle Pliocene Warm Period and the Middle Miocene Thermal Maximum, during which CO_2 was perhaps modestly elevated (400–600 ppm) and for which paleoclimate reconstructions are likely better, versus more ancient time slices, during which CO_2 may have been substantially higher but for which paleoclimate data are more sparse and for which there are larger uncertainties associated with other factors that influence Earth's surface temperature, including continental configuration and ocean circulation, global topography and solar luminosity. Further, ESS may vary as a function of $[CO_2]_{atm}$ and may be higher for icehouse climates than for greenhouse climates (Park and Royer, 2011). It should be noted that the results presented in Fig. 3 do not consider secular variation in $[CO_2]_{atm}$ which likely occurred to some degree during any time slice of interest. Secular variation in $[CO_2]_{atm}$ would increase the uncertainty associated with ESS. Nonetheless, these results suggest that averaging of >10 paleosols will likely result in useful constraints on ESS. Averaging results from >30 paleosols may not substantially reduce ESS uncertainty, except for Vertisols. Averaging results from <5 paleosols, given current constraints on $S(z)$ will likely result in very large errors on ESS. Similar adjacent paleosols in the same section should probably not be considered independent for the purposes of this type of analysis because such paleosols likely formed under similar conditions and therefore may be better considered as replicates than as being truly independent of one another. Even so, 10–30 independent paleosols is a feasible number and warrants targeted study of paleosols that formed during warm episodes of the Cenozoic and earlier.

5. Recommended procedure

The following procedure is recommended for reconstructing atmospheric CO_2 from paleosol carbonates, in addition to those described by Cotton and Sheldon (2012). The following data should be reported in addition to best values and standard deviations for the variables in Eq. (1): detailed paleosol descriptions, interpretation of soil order including the criteria used, and measurements of depth to Bk. If depth to Bk is used to assign $S(z)$, the criteria used to identify the paleosurface should be reported or the absence of a clear paleosurface should be indicated. Reporting of CIA-K or CALMAG is also encouraged. These data will allow for future improvements and comparison among studies. The carbon isotope composition of organic matter in each paleosol, preferably organic matter occluded in carbonate nodules, should be measured (Cerling, 1992; Cotton and Sheldon, 2012). The measurement of multiple samples from each paleosol, collected along transects parallel to the paleosurface will result in the most representative atmospheric CO_2 concentrations. Gaussian or Monte Carlo error bars should be reported along with best values for CO_2.

6. Conclusions

Gaussian and Monte Carlo error propagation yield similar results. For the Miocene paleosols considered here, Monte Carlo-simulated distributions of $[CO_2]_{atm}$ are slightly skewed toward high values. The approaches for assigning $S(z)$ should be tested using late Pleistocene and Holocene buried soils as they result in significantly different values of $[CO_2]_{atm}$ for the Miocene paleosols considered here. Averaging among >10 independent paleosols is likely to result in useful constraints on Earth system sensitivity. Given the abundance of Neogene paleosols in the rock record, such averaging should be feasible.

Acknowledgments

The authors would like to thank two anonymous reviewers who helped improve this paper.

Appendix A. Supplementary data

Supplementary data to this article can be found online at http://dx.doi.org/10.1016/j.palaeo.2014.04.012.

References

Badger, M.P.S., Lear, C.H., Pancost, R.D., Foster, G.L., Bailey, T.R., Leng, M.J., Abels, H.A., 2013. CO_2 drawdown following the middle Miocene expansion of the Antarctic Ice Sheet. Paleoceanography 28, 42–53.

Beerling, D.J., Fox, A., Anderson, C.W., 2009. Quantitative uncertainty analyses of ancient atmospheric CO_2 estimates from fossil leaves. Am. J. Sci. 309, 775–787.

Berner, R.A., 2006. Geocarbsulf: a combined model for Phanerozoic atmospheric O_2 and CO_2. Geochim. Cosmochim. Acta 70, 5653–5664.

Bestland, E.A., Krull, E.S., 1999. Palaeoenvironments of Early Miocene Kisingiri volcano *Proconsul* sites: evidence from carbon isotopes, palaeosols and hydromagmatic deposits. J. Geol. Soc. Lond. 156, 965–976.

Bowen, G.J., Beerling, D.J., 2004. An integrated model for soil organic carbon and CO_2: implications for paleosol carbonate pCO_2 paleobarometry. Glob. Biogeochem. Cycles 18, GB1026.

Breecker, D.O., 2013. Quantifying and understanding the uncertainty of atmospheric CO2 concentrations determined from calcic paleosols. Geochem. Geophys. Geosyst. 14, 3210–3220.

Breecker, D., Sharp, Z.D., McFadden, L., 2009. Seasonal bias in the formation and stable isotope composition of pedogenic carbonate in modern soils from central New Mexico, USA. Geol. Soc. Am. Bull. 121, 630–640.

Breecker, D.O., Sharp, Z.D., McFadden, L.D., Breecker, D.O., Sharp, Z.D., McFadden, L.D., 2010. Atmospheric CO_2 concentrations during ancient greenhouse climates were similar to those predicted for A.D. 2100. Proc. Natl. Acad. Sci. U. S. A. 107, 576–580.

Breecker, D.O., Yoon, J., Michel, L.E., Dinka, T.M., Driese, S.G., Mintz, J.S., Nordt, L.C., Romanak, K.D., Morgan, C.L.S., 2013. CO_2 concentrations in Vertisols: seasonal variability and shrink-swell. In: Driese, S.G., Nordt, L.C., McCarthy, P.J. (Eds.), New Frontiers in Paleopedology and Terrestrial Paleoclimatology: Paleosols and Soil Surface Analog Systems, vol.104. SEPM.

Caballero, R., Huber, M., 2013. State dependent climate sensitivity in past warm climates and its implications for future climate projections, v 110. pp. 14162–14167.

Cerling, T.E., 1991. Carbon dioxide in the atmosphere: evidence from Cenozoic and Mesozoic paleosols. Am. J. Sci. 291, 377–400.

Cerling, T.E., 1992. Use of carbon isotopes in paleosols as an indicator of the $p(CO_2)$ of the paleoatmosphere. Glob. Biogeochem. Cycles 6, 307–314.

Cerling, T.E., 1999. Stable carbon isotopes in palaeosol carbonates. In: Thiry, M., Coincon, R.S. (Eds.), Palaeoweathering, Palaeosurfaces and Related Continental Deposits. Special Publication of the International Association of Sedimentologists, vol. 27, pp. 43–60.

Charney, J.G., 1979. Carbon Dioxide and Climate: A Scientific Assessment. National Academy of Science, Washington D.C. p. 22.

Clifford, A.A., 1973. Multivariate Error Analysis: A Handbook or Error Propagation and Calculation in Many-parameter Systems. Applied Science Publishers, London.

Cotton, J.M., Sheldon, N.D., 2012. New constraints on using paleosols to reconstruct atmospheric pCO_2. Geol. Soc. Am. Bull. 124, 1411–1423.

Cotton, J.M., Jeffery, M.L., Sheldon, N.D., 2013. Climate controls on soil respired CO_2 in the United States: implication for 21st century weathering rates in temperate and arid ecosystems. Chem. Geol. 358, 37–45.

Drake, R.E., Van Couvering, J.A., Pickford, M.H., Curtis, G.H., Harris, J.A., 1988. New chronology for the Early Miocene mammalian faunas of Kisingiri western Kenya. J. Geol. Soc. Lond. 145, 479–491.
Dworkin, S.I., Nordt, L., Atchley, S., 2005. Determining terrestrial paleotemperatures using the oxygen isotopic composition of pedogenic carbonate. Earth Planet. Sci. Lett. 237, 56–68.
Feng, X., Peterson, J.C., Quideau, S.A., Virginia, R.A., Graham, R.C., Sonder, L.J., Chadwick, O. A., 1999. Distribution, accumulation and fluxes of soil carbon in four monoculture lysimeters at San Dimas Experimental Forest, California. Geochim. Cosmochim. Acta 63, 1319–1333.
Foster, G.L., Lear, C.H., Rae, J.W.B., 2012. The evolution of pCO_2, ice volume and climate during the middle Miocene. Earth Planet. Sci. Lett. 341–344, 243–254.
Fox, D., Koch, P.L., 2003. Tertiary history of C_4 biomass in the Great Plains, USA. Geology 31, 809–812.
Gallagher, T.M., Sheldon, N.D., 2013. A new paleothermometer for forest paleosols and its implication for Cenozoic climate. Geology 41, 647–650.
Ghosh, P., Adkins, J., Affek, H., Balta, B., Guo, W., Schauble, E.A., Schrag, D., Eiler, J.M., 2006. $^{13}C-^{18}O$ bonds in carbonate minerals: a new kind of paleothermometer. Geochim. Cosmochim. Acta 70, 1439–1456.
Hansen, J., Sato, M., Kharecha, P., Beerling, D.J., Berner, R.A., Masson-Delmonte, V., Pagani, M., Raymo, M., Royer, D.L., Zachos, J.C., 2008. Target atmospheric CO2: where should humanity aim. Open Atmos. Sci. J. 2, 217–231.
Hough, B.G., Fan, M., Passey, B.H., 2014. Calibration of the clumped isotope geothermometer in soil carbonate in Wyoming and Nebraska, USA: implication for paleoelevation and paleoclimate reconstruction. Earth Planet. Sci. Lett. 391, 110–120.
Indermühle, A., Stocker, T.F., Joss, F., Fischer, H., Smith, H.J., Wahlen, M., Deck, B., Mastroianni, D., Tschumi, J., Blunier, T., Meyer, R., Stauffer, B., 1999. Holocene carbon-cycle dynamics based on CO_2 trapped in ice at Taylor Dome, Antarctica. Nature 398, 121–126.
Kent-Corson, M.L., Sherman, L.S., Mulch, A., Chamberlain, C.P., 2006. Cenozoic topographic and climatic response to changing tectonic boundary conditions in western North America. Earth Planet. Sci. Lett. 252, 453–466.
Kürschner, W.M., 1996. Leaf stomata as biosensors of plaeoatmospheric CO2 levels. LPP Contributions Series, 5, pp. 1–153.
Kürshcner, W.M., Kvacek, Z., Dilcher, D.L., 2008. The impact of Miocene atmospheric carbon dioxide fluctuations on climate and the evolution of terrestrial ecosystems. Proceedings of the National Academy of Science USA, pp. 449–453.
Lunt, D.J., Haywood, A.M., Schmidt, G.A., Salzmann, U., Valdes, P.J., Dowsett, H.J., 2010. Earth system sensitivity inferred from Pliocene modelling and data. Nat. Geosci. 3, 60–64.
Montañez, I.P., 2013. Modern soil system constraints on reconstructing deep-time atmospheric CO2. Geochim. Cosmochim. Acta 101, 57–75.
Montañez, I.P., Tabor, N.J., Niemeler, D., DiMichele, W.A., Frank, T.D., Fielding, C.R., Isbell, J. L., Birgenheier, L.P., Rygel, M.C., 2007. CO_2-forced climate and vegetation instability during late Paleozoic deglaciation. Science 315, 87–91.
Mora, C.I., Sheldon, B.T., Elliott, W.C., Driese, S.G., 1998. An oxygen isotope study of illite and calcite in three Appalachain Paleozoic vertic paleosols. J. Sediment. Res. 68, 456–464.
Naish, T., Zwartz, D., 2012. Paleoclimate: looking back to the future. Nat. Clim. Chang. 2, 317–318.
Nordt, L., Driese, S.G., 2010. New weathering index improves paleorainfall estimates from Vertisols. Geology 38, 407–410.
Park, J., Royer, D.L., 2011. Geologic constraints on the glacial amplication of Phanerozoic climate sensitivity. Am. J. Sci. 311, 1–26.
Passey, B.H., Cerling, T.E., Perkins, M.E., Voorhies, M.R., Harris, J.M., Tucker, S.T., 2002. Environmental change in the Great Plains: an isotopic record from fossil horses. J. Geol. 110, 123–140.
Passey, B.H., Levin, N.E., Cerling, T.E., Brown, F.H., Eiler, J.M., 2010. High temperature environments of human evolution in East Africa based on bond ordering in paleosol carbonates. Proc. Natl. Acad. Sci. U. S. A. 107, 11245–11249.
Peters, N.A., Huntington, K.W., Hoke, G.D., 2013. Hot or not? Impact of seasonally variable soil carbonate formation on paleotemperature and O-isotope records from clumped isotope thermometry. Earth Planet. Sci. Lett. 361, 208–218.
Pierrehumbert, R.T., 2013. Hot climates, high sensitivity. Proc. Natl. Acad. Sci. U. S. A. 110, 14118–14119.
Quade, J., Eiler, J., Daëron, M., Achyuthan, H., 2013. The clumped isotope geothermometer in soil and paleosol carbonate. Geochim. Cosmochim. Acta 105, 92–107.
Retallack, G.J., 2005. Pedogenic carbonate proxies for amount and seasonality of precipitation in paleosols. Geology 33, 333–336.
Retallack, G.J., 2007. Cenozoic paleoclimate on land in North America. J. Geol. 115, 271–294.
Retallack, G.J., 2009a. Greenhouse crises of the past 300 million years. Geol. Soc. Am. Bull. 121, 1441–1455.
Retallack, G.J., 2009b. Refining a pedogenic-carbonate CO_2 paleobarometer to quantify a middle Miocene greenhouse spike. Palaeogeogr. Palaeoclimatol. Palaeoecol. 281, 57–65.
Retallack, G.J., Wynn, J.G., Fremd, T.J., 2004. Glacial–interglacial-scale paleoclimatic changes without large ice sheets in the Oligocene of central Oregon. Geology 32, 297–300.
Romanek, C.S., Grossman, E.L., Morse, J.W., 1992. Carbon isotopic fractionation in synthetic aragonite and calcite — effect of temperature and precipitation rate. Geochim. Cosmochim. Acta 56, 419–430.
Royer, D.L., Wing, S.L., Beerling, D.J., Jolley, D.W., Koch, P.L., Hickey, L.J., Berner, R.A., 2001. Paleobotanical evidence for near present-day levels of atmospheric CO_2 during part of the Tertiary. Science 292, 2310–2313.
Royer, D.L., Pagani, M., Beerling, D.J., 2012. Geobiological constraints on Earth system sensitivity to CO_2 during the Cretaceous and Cenozoic. Geobiology 10, 298–310.
Schaller, M.F., Wright, J.D., Kent, D.V., 2011. Atmospheric pCO_2 perturbations associated with the Central Atlantic Magmatic Province. Science 331, 1404–1409.
Schmidt, G.A., Annan, J.D., Bartlein, P.J., Cook, B.I., Guilyardi, E., Hargreaves, J.C., Harrison, S. P., Kageyama, M., Legrande, A.N., Konecky, B., Lovejoy, S., Mann, M.E., Masson-Delmotte, V., Risi, C., Thompson, D., Timmerann, A., Tremblay, L.-B., Yiou, P., 2013. Using paleo-climate comparisons to constrain future projections in CMIP5. Clim. Past Discuss. 9, 775–835.
Sheldon, N.D., Retallack, G.J., Tanaka, S., 2002. Geochemical climofunctions from North American soils and application to plaeosols across the Eocene/Oligocene boundary in Oregon. J. Geol. 110, 687–696.
Solomon, S., Qin, D., Manning, M., Alley, R.B., Berntsen, T., Bindoff, N.L., Chen, Z., Chidthaisong, A., Gregory, J.M., Hegerl, G.C., Heimann, M., Hewitson, B., Hoskins, B.J., Joos, F., Jouzel, J., Kattsov, V., Lohmann, U., Matsuno, T., Molina, M., Nicholls, N., Overpeck, J., Raga, G., Ramaswamy, V., Ren, J., Rusticucci, M., Somerville, R., Stocker, T.F., Whetton, P., Wood, R.A., Wratt, D., 2007. Technical Summary. In: Solomon, S., Qin, D., Manning, M., Chen, Z., Marquis, M., Averyt, K.B., Tignor, M., Miller, H.L. (Eds.), Climate Change 2007: The Physical Science Basis. Contribution of Working Group I to the Fourth Assessment Report of the Intergovernmental Panel on Climate Change. Cambridge University Press, Cambridge, UK and New York, USA.
Staff, S.S., 2010. Keys to Soil Taxonomy, 11th ed. USDA-Natural Resources Conservation Service, Washington D.C.
Stocker, T., Qin, D.-H., Plattner, G.K., 2013. Climate change 2013: the physical science basis. Contribution of Working group 1 to the Fifth Assessment Report of the Intergovernmental Panel on Climate Change: Cambridge, UK and New York, USA.
Tans, P., Keeling, R., 2013. Recent Mauna Loa CO2 on NOAA/ESRL (website (http://www.esrl.noaa.gov/gmd/ccgg/trends/) Volume 2013).
Tipple, B.J., Meyers, S.R., Pagani, M., 2010. Carbon isotope ratio of Cenozoic CO2: a comparative evaluation of available geochemical proxies. Paleoceanography 25, PA3202.
Torn, M.S., Lapenis, A.G., Timofeev, A., Fischer, M.L., Babikov, B.V., Harden, J.W., 2002. Organic carbon and carbon isotope sin modern and 100-year-old-soil archives of the Russian steppe. Glob. Chang. Biol. 8, 941–953.
Tripati, A.K., Roberts, C.D., Eagle, R.A., 2009. Coupling of CO2 and ice sheet stability of major climate transitions of the last 20 million years. Science 326, 1394–1397.
Van Der Burgh, J., Visscher, H., Dilcher, D.L., Kürschner, W.M., 1993. Paleoatmospheric signatures in Neogene fossil leaves. Science 260, 1788–1790.
Wynn, J.G., Bird, M.I., 2007. C_4-derived soil organic carbon decomposes faster than its C_3 counterpart in mixed C_3/C_4 soils. Glob. Chang. Biol. 13, 2206–2217.
Wynn, J.G., Bird, I.M., Wong, V.N.L., 2005. Rayleigh distillation and the depth profile of $^{12}C/^{13}C$ ratios of soil organic carbon from soils of disparate texture in Iron Range National Park, Far North Queensland, Australia. Geochim. Cosmochim. Acta 69, 1961–1973.
Zhang, Y.G., Pagani, M., Liu, Z., Bohaty, S.M., DeConto, R., 2013. A 40-million-year history of atmospheric CO_2. Phil. Trans. R. Soc. A 371, 20130096.